

DOI: 10.17148/IJIREEICE.2025.131016

# An Optimisation Framework for Induction Motor Power in Electric Vehicles Using Fuzzy Logic Control

#### RAYAVARAPU SAI KIRAN<sup>1</sup>, A. CHAKRADHAR<sup>2</sup>

PG Student, Department of Electrical Engineering, Sankethika Vidya Parishad Engineering College, Andhra Pradesh, India<sup>1</sup>

Assistant Professor, Department of Electrical Engineering, Sankethika Vidya Parishad Engineering College,

Andhra Pradesh, India<sup>2</sup>

Abstract: Energy efficiency plays a vital role in electric and hybrid vehicles (EVs) due to their limited energy storage capacity. Besides its excellent stability and low cost, minimizing losses enhances the efficiency of the induction motor. Furthermore, when operating below its maximum load, it may consume more power than necessary for its tasks. This study proposes a fuzzy logic control (FLC)-based method for applications in electric vehicles. The FLC controller is capable of conserving additional power and improving the initial current amplitude. The performance of the control was validated through simulation using the MATLAB/SIMULINK software program. The simulation results indicate a swift rejection of disturbances impacting the system and demonstrate superior performance outcomes in the time-domain response compared to the conventional proportional integral derivative controller. Consequently, the core losses of the induction motor are significantly reduced, thereby enhancing the efficiency of the driving system.

#### I. INTRODUCTION

The significant rise in fossil fuel usage, particularly over the last few decades, has led to an increase in atmospheric CO2 levels. In light of the escalating concerns regarding climate change and rising sea levels due to global warming, there is an urgent necessity for global efforts to reduce carbon dioxide emissions. Enhancing vehicle fuel efficiency is crucial, as transportation accounts for approximately 20% of total carbon dioxide emissions [1-6]. Electric vehicles (EVs) offer numerous advantages, including being quieter, more environmentally friendly, more efficient, and generally less reliant on fuel [7]. The choice of electric machine greatly influences the cost and efficiency of the drive. Electric motors are essential components in all drive systems, including hybrid and EV models [8]. The primary types of machines that can be utilized in electric vehicles (EVs) are induction motors (IMs) and synchronous motors [9]. The following propulsion characteristics should be integrated into the EV-drive motor [7, 10–12]: (I) high efficiency to enhance driving range; (ii) high torque density to ensure adequate driving force during starting, climbing, and acceleration; (iii) the capability to manage flow effectively to extend the range of static power speeds. Due to its durability, affordability, and minimal maintenance needs, the IM is the preferred choice for EVs and is more commonly employed for traction drives [13–16]. However, its losses are considerably higher in EV applications [17, 18], which leads to a decrease in the machine's efficiency. The primary challenges in integrating these vehicles into the transportation system include their increased weight, low energy density, prolonged battery life, and extended charging times [19]. Consequently, the effective use of energy is crucial for the operation of electric vehicles [20–22]. It is generally acknowledged that proportional integral derivative (PID) control, commonly used in various industrial drives, is one of the most prevalent components. Additionally, PID controllers are utilized in industrial settings and form part of the majority of control loops currently implemented [23, 24]. A significant decline in performance may occur when operating conditions change, as components may become outdated or the working environment may shift [25]. Fuzzy logic control (FLC) represents an intelligent control method that can provide superior performance compared to precise analytical modeling of a controlled system, as it is less ambiguous and more user-friendly [26-28]. The FLC framework offers numerous strategy rules that utilize linguistic tags in a more straightforward manner. Several other investigations into energy demand control in electric vehicles have adopted this approach [7]. FLC operates in a model-free manner, meaning it does not rely on a mathematical model of the controlled system [28, 29]. Therefore, the FLC system controller should be designed with adaptive features to enhance the performance of the electric vehicle traction when the system encounters areas with persistent errors. Other considerations in FLC involve identifying suitable trade-offs between minimal overshoot, minimal steady-state error, and rapid rise time [30]. Nevertheless, the objective of the current design methodologies is to minimize steady-state losses [31, 32]. During transit, the machine may experience high and excessive current peak losses with variable flow linkages, particularly when high stability efficiency is the design objective for conventional induction machines. Consequently, the



#### DOI: 10.17148/IJIREEICE.2025.131016

losses associated with transient machines that occur during the highly dynamic driving cycle frequently experienced by the electric vehicle traction motor drive are the primary focus of this article. A variety of alternative control structures for electric vehicle (EV) applications have been documented in the literature. These include simple linear methods such as direct torque and field-oriented control [8, 33], sliding mode control [36], and other control strategies [34, 35]. The finite element approach [17] is employed to reduce secondary winding harmonic losses, utilizing the golden section method [33], alongside a model reference adaptive system featuring an optimal base power scheme. Additionally, the adaptive quadratic interpolation-based search controller (SC) is utilized to optimize the loss of the induction motor (IM) drive [20], while a fuzzy controller with nine rules is implemented for slip control, generating frequency by using the variation in speed error as an input. For electric vehicle applications, this paper proposes a fuzzy logic controller (FLC)-based approach. Subsequently, a comparison between the controllers (PID and FLC) is presented, focusing on their impact on the performance of the induction motor (IM). The key findings from this study can be summarized as follows: Efficiency serves as a metric for energy expenditure, with the primary objective being the reduction of the drive's life cycle cost at anticipated speeds and beyond. The efficiency of the inverter is contingent upon the overall driving efficiency.

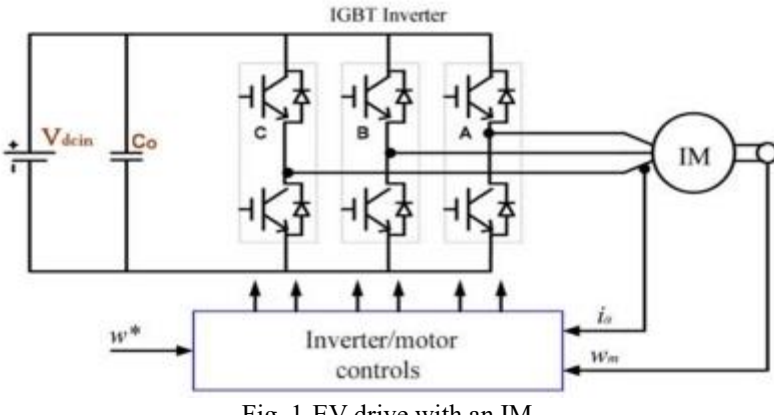


Fig. 1 EV drive with an IM

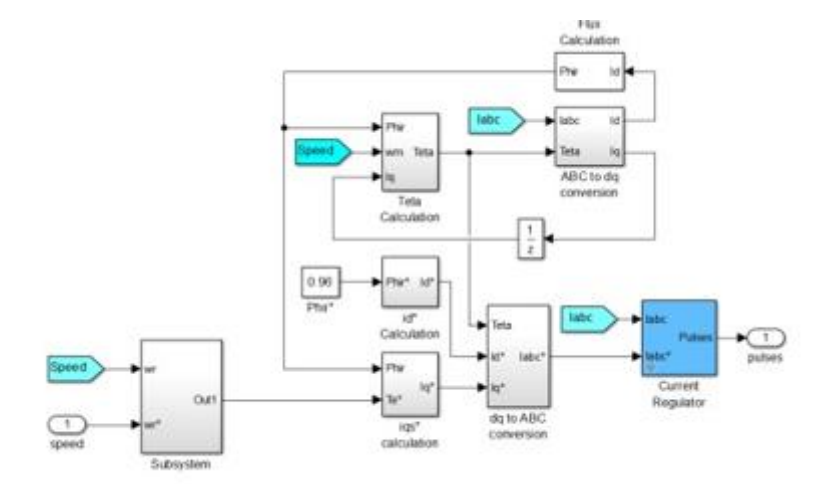


Fig. 2 Control system of IM

The remainder of this document is organized as follows: Section 2 provides a description of the circuit, while Section 3 outlines the control theory. Section 4 delves into the efficiency of the IM drive and the calculations of power loss. The simulation results are presented in Section 5, followed by the experimental results in Section 6, and the conclusion is drawn in Section 7.

#### II. CIRCUIT DESCRIPTION

As illustrated in Fig. 1, a battery-electric vehicle (BEV) is defined as a vehicle powered by electricity, consisting of three fundamental components: an electric motor system, typically a single electrical machine (usually a three-phase AC), which connects to the wheels via the differential and gearbox. The second component is a battery that chemically stores energy. This battery interfaces with the device through an electronic DC/AC power adapter, along with the control system. Lastly, the electric machine is outfitted with a three-phase frequency and voltage control system that modifies its



#### DOI: 10.17148/IJIREEICE.2025.131016

operation based on the driver's requirements. This system is linked to the accelerator and/or brake pedals. The three-phase electric machine depicted in Fig. 1 is responsible for providing traction to the wheels. The electric motor shaft adjusts its high speed to match the low speed of the differential through a gear ratio. The left and right wheels receive power from the wheels. An inverter, which converts the DC electricity from the battery into three-phase AC voltage, governs the speed of the machine. When evaluating the power consumption of an electric vehicle (EV) that is not connected to the grid, it is essential to consider component losses. Our commitment is to create suitable controllers for feedback to ensure the EV system operates as required. By employing FLC methods, a controller that is sufficiently powerful, flexible, and adaptive can be implemented for EV applications.

#### III. CONTROL METHOD

#### A. Conventional PID control

In the initial design approach, a conventional PID controller is employed to manage the speed of an indirect field-oriented IM order. Furthermore, the initial conditions are analyzed. As illustrated, a phase-locked loop algorithm that synchronizes with the utility current regulator and the (direct-quadrature-zero) transformation equations are incorporated into the proposed control system depicted in Fig. 2. The phase currents (ia, ib, and ic) are converted from a-b-c coordinates into a d-q frame. The subsequent transformations can be utilized to define the components of d-q:

$$\begin{bmatrix} i_d \\ i_q \end{bmatrix} = \sqrt{\frac{2}{3}} \begin{bmatrix} \sin(\omega t) & \sin(\omega t - \frac{2\pi}{3}) & \sin(\omega t + \frac{2\pi}{3}) \\ \cos(\omega t) & \cos(\omega t - \frac{2\pi}{3}) & \cos(\omega t + \frac{2\pi}{3}) \end{bmatrix} \times \begin{bmatrix} i_{sa} \\ i_{sb} \\ i_{sc} \end{bmatrix}$$
(1)

The computation of active and reactive power now incorporates average and oscillation components. However, to derive the average components for the outputs of the PID control loops, two external PID control loops are employed for both reactive and active power. Figure 3 illustrates a block diagram of the conventional PID control. Based on the subsequent conversions, this PID produces the active current reference (id\*) and the reactive current reference.

(2)  

$$i_{d}^{*} = k_{p}(P_{ref} - P) + k_{i} \int (P_{ref} - P) dt$$
(3)  

$$i_{q}^{*} = k_{p}(Q_{ref} - Q) + k_{i} \int (Q_{ref} - Q) dt$$

If ki represents the fundamental constant and kp denotes the proportional constant for the utilized PID controllers. The reference for charging power is termed Pref, while the reactive power required by the AC source is referred to as Oref

The integration of the inner current loop and the outer voltage loop facilitates the control mechanism. The outer loop generates current when the actual current is compared to the current reference, which in turn governs the inner loop. Consequently, by evaluating the measured line currents obtained through the park transformation, the internal PID loops are established. To derive the operating ratios in the d–q coordinates, the results (ed and eq) are initially aggregated based on the disengagement conditions and subsequently normalized by the DC voltage as follows:

The duty ratios in the frame coordinates (a, b, and c) can be derived through inverse matrix transformation and are expressed as follows:

$$\begin{bmatrix}
D_a \\
D_b \\
D_c
\end{bmatrix} = \sqrt{\frac{2}{3}} \begin{bmatrix} \sin(\omega t) & \cos(\omega t) \\
\sin(\omega t - \frac{2\pi}{3}) & \cos(\omega t - \frac{2\pi}{3}) \\
\sin(\omega t + \frac{2\pi}{3}) & \cos(\omega t + \frac{2\pi}{3}) \end{bmatrix} \times \begin{bmatrix} d_d \\ d_q \end{bmatrix} \tag{5}$$

#### B. Description of suggested FLC

Addressing this issue remains difficult due to the non-linear properties of AC motors, especially the squirrel cage induction motor (SCIM), as various parameters (mainly rotor resistances) fluctuate based on the operational environment.



#### DOI: 10.17148/IJIREEICE.2025.131016

As a result, for electric vehicle (EV) applications, it is essential to implement an effective intelligent fuzzy logic controller (FLC) [37] to enhance the traditional control technology (PID). In the design of a fuzzy system, the key variables to take into account include:

- (i) the formulation of fuzzy rules by experts in the field for particular control problems;
- (ii) the choice and fine-tuning of membership functions; and
- (iii) the determination of scaling factors.

The fundamental FLC for EV applications was developed utilizing the second design approach. EV applications represent a well-established domain for variable structure control units, recognized for their stability and durability. Figure 4 illustrates a typical FLC.

Fuzzy logic serves as a mathematical approach that enhances voltage, frequency, and current regulation for adjustable speed drives. It is applicable in EV scenarios to address challenges when non-linearity and its dynamic characteristics are too complex for conventional control methods to manage. Such challenges are prevalent in motor control.

#### C. Speed control FLC

In the context of motor speed regulation, Fuzzy Logic Control (FLC) necessitates two input parameters: the motor speed error (we) and its derivative, representing the speed variation error ( $\Delta$ we). This encompasses both speed and the error in speed. One method to elucidate the concept of variation error is as follows:

(6) 
$$we = w_{\text{ref}}^* - w_{\text{act}}$$

where the terms "w\*ref" and "wact" stand for the actual/measured motor speed and the reference motor speed, respectively:

$$\frac{\mathrm{d}we}{\mathrm{d}t} = \frac{\Delta we}{T_s}$$

(7)

The incremental change in the control signal  $\Delta u$  is the controller output. It is possible to obtain the control signal by

$$\Delta u = \Delta t_e^* = k_1 \cdot we + k_2 \cdot \Delta we$$

where k1 and k2 represent the previous and current states of the system, respectively. As depicted in Fig. 5, the normalized domain [-1, 1] establishes the universe of discourse for all membership functions pertaining to the controller inputs, namely we and  $\Delta$ we, as well as the output,  $\Delta$ u.

Fuzzy logic membership functions have been divided into five membership functions (MF) for the inputs and five MF for the output fuzzy sets, as illustrated in Figure 5.

In this framework, two input variables are associated with a single output variable through a Mamdani fuzzy inference method. The error (we) signifies the differences between the two input variables, which include the recorded speed, the desired speed (set-point), and the change in error ( $\Delta$ we). In Fig. 4, the scaling factors Ge, Gde, and Gu perform the normalization and denormalization of the individual variables of a conventional control gain.

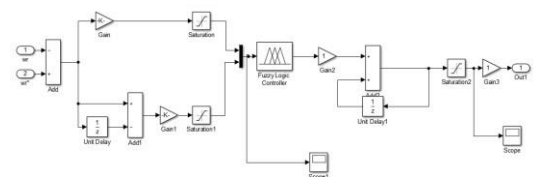


Fig. 4 Detailed construction of the fuzzy controller

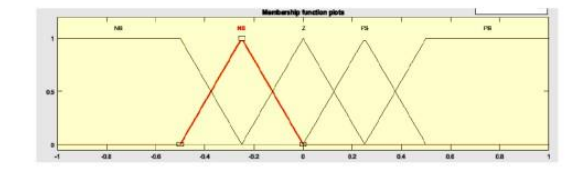


Fig. 5 Membership function of FLC (we), ( $\Delta$ we), ( $\Delta$ u)



#### DOI: 10.17148/IJIREEICE.2025.131016

Table 1 Rules of the FLC

Δwe	we				
	NB	NS	Z	PS	PB
NB	NB	NB	NS	NS	Z
NS	NB	NS	NS	Z	PS
Z	NS	NS	Z	PS	PS
PS	NS	Z	PS	PS	PB
PB	Z	PS	PS	PB	PB

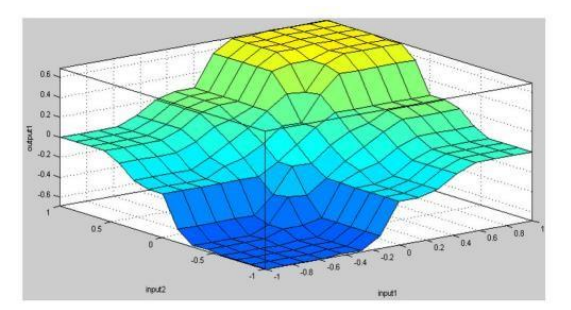


Fig. 6 Crisp in./out. Map

The values of these measurement factors are contingent upon the initial error, with Ge, Gde, and Gu representing the error measurement, error variation, and FLC output factors, respectively. As shown in Fig. 5, constrained models are utilized to minimize the error and the variance in the error between the input and output functions of the FLC, which range from (1, -1), while the FLC rules are Logged into Table 1. Instead of merely utilizing NB, NS, Z, PS, and PB, this feature proposes that a more precise continuous control rule can be developed by interpolating the fundamental table of rules which represent, in that sequence, negative big, negative small, zero, positive small, and positive big. This time, symmetrical triangles with an equal base and 50% overlap with adjacent MFs are chosen, with the exception of two obscure groups at the outer edges (trapezoidal MFs are selected). Each variable consists of five fuzzy subsets, as shown in Table 1, resulting in a total of 25 possible rules. A typical rule is stated as follows: "If e is NB and de is PB, then u is Z." Due to the perturbation method altering the motor speed and output power, it is essential to implement speed correction control. The output rotor speed of the motor must be maintained as consistently as possible. Figure 6 illustrates the input/output mapping for the FLC. By employing this fuzzy controller in the outer loop and utilizing the speed error along with the variation of error as input signals to formulate the corresponding control terms, it is possible to achieve smooth torque and enhanced system performance for electric vehicle applications.

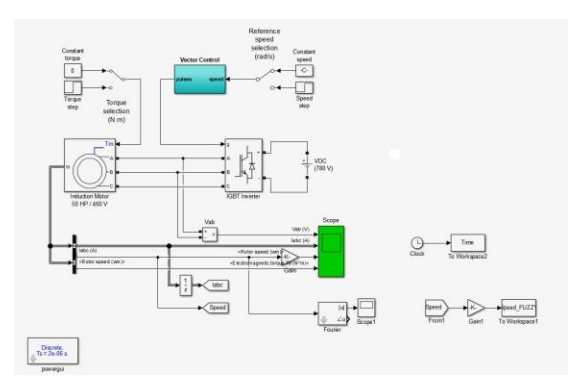


Fig. 8 MATLAB model of three-phase IM

#### IV. POWER LOSS CALCULATION AND EFFICIENCY OF INDUCTION MOTOR DRIVE

To verify the assessed efficiency, the subsequent power losses of the proposed control scheme are analyzed for a worst-case scenario under full load. This section presents the complete array of provided and calculated parameters as shown in Table 2. The typical values from the datasheet serve as the source for these parameters. Subsequently, several computed parameters will be exhibited. Reference [38] indicates that the stray losses are negligible. The three-phase inductive motor consumes 60 A at a power factor of 0.85 lagging under full load current (FLC) conditions and 62.6 A at a power factor of 0.85 lagging when operating with proportional-integral-derivative (PID) control. The input power losses can be estimated as

International Journal of Innovative Research in Electrical, Electronics, Instrumentation and Control Engineering
Impact Factor 8.414 

Refereed journal 

Vol. 13, Issue 10, October 2025

DOI: 10.17148/IJIREEICE.2025.131016

$$P_{\text{In}} = \sqrt{3} \times V_{\text{L}} I_{\text{L}} \cos \theta = 3 \times V_{\text{ph}} I_{\text{ph}} \cos \theta$$
(9)

It is estimated that the copper losses in the stator amount to 2 kW, while the core losses are 1.8 kW. The air-gap power losses can be approximated as

$$P_{AG} = P_{In} - (P_{SCL} + P_{Core})$$

$$= P_{Conv} + P_{RCL} = 3I_2^2 \frac{R_2}{S} = \frac{P_{RCL}}{S}$$
(10)

Table 2 Given and calculated parameters

Item	Symbol	Value
voltage (line-to-line)	V <sub>L</sub>	460 V
frequency	F	60 Hz
number of poles	P	4
power factor	PF	0.85 lagging
three-phase IM is drawing (PID)	<i> </i> _	62.6 A
three-phase IM is drawing (FLC)	<i>I</i> L	60 A
stator copper losses (PID)	PSCL	2 kW
stator copper losses (FLC)	PSCL	1.8 kW
rotor copper losses (PID)	P <sub>RCL</sub>	700 W
rotor copper losses (FLC)	PRCL	500 W
core losses	PCore	1.8 kW
friction and windage losses	$P_{F\&W}$	600 W

Table 3 Results of power losses analysis under full load and efficiency estimation of IM drive using PID and FLC

Item	Power losses calculation	PID	FLC
input power	$P_{\rm In} = \sqrt{3} \times V_{\rm L} I_{\rm L} \cos \theta$	42.395 kW	40.634 kW
	$= 3 \times V_{\rm ph}I_{\rm ph}\cos\theta$		
air-gap power losses	$P_{\rm AG} = P_{\rm In} - (P_{\rm SCL} + P_{\rm Core})$	38.595 kW	37.034 kW
converted power losses	$P_{\rm Conv} = P_{\rm AG} - P_{\rm RCL}$	37.895 kW	36.534 kW
output power	$P_{\text{out}} = P_{\text{Conv}} - (P_{\text{f\&w}} + P_{\text{stray}})$	37.295 kW	35.934 kW
efficiency	$\eta = \frac{P_{\rm out}}{P_{\rm in}} \times 100$	87.97%	88.43%

$$P_{\text{Conv}} = P_{\text{AG}} - P_{\text{RCL}}$$

$$= 3I_2^2 \frac{R_2(1-S)}{S} = \frac{P_{\text{RCL}}(1-S)}{S}$$
(11)

The sole rotor copper losses factored into the power conversion calculation amount to 700 W. It is feasible to approximate the converted power losses as

$$P_{\text{Conv}} = (1 - S)P_{\text{AG}} \tag{12}$$

The calculation takes into account the premise that stray losses are negligible, indicating that both the friction and windage losses amount to 600 W each. A method to assess the output power losses is presented in Table 3.



DOI: 10.17148/IJIREEICE.2025.131016

$$P_{\text{Out}} = P_{\text{Conv}} - (P_{f+w} + P_{stray})$$
(13)

The efficiency of the IM drive concerning load percentage is illustrated in Fig. 7. This figure indicates that energy efficiency increases when the IM operates at optimal performance. By comparing the results achieved by the controller tuned with several established tuning rules to those generated by the proposed rules, it is evident that the suggested approach yields superior performance.

#### V. SIMULATION RESULTS

Two instances have been analyzed in the simulation, utilizing the Simulink and power sum toolboxes of the MATLAB software, as illustrated in Fig. 8. The initial case study employs a PID controller to operate a 50-horsepower inline motor. During the first five seconds of its operation, three-phase voltage and current measurements are recorded and analyzed. Additionally, the torque resulting from the acceleration curve is also examined. In the subsequent scenario, a Fuzzy Logic Controller (FLC) is implemented to directly control the motor. The response of the PID controller is compared with that of the FLC, with the results presented in Figs. 9–11.

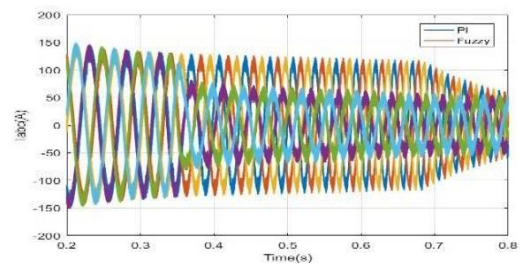


Fig. 9 Three-phase stator current of PID and FLC models (A)

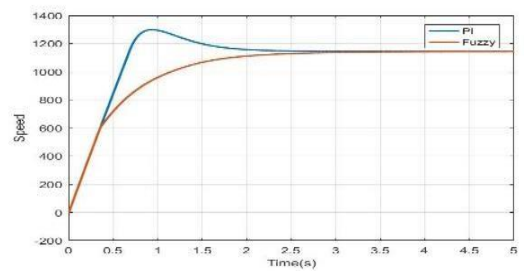


Fig. 10 Simulation response of PID and FLC for rotor speed (rpm)

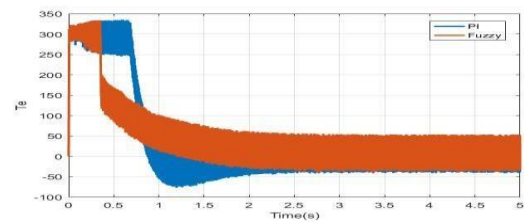


Fig. 11 Simulation response of PID and FLC for electromagnetic torque (N m)

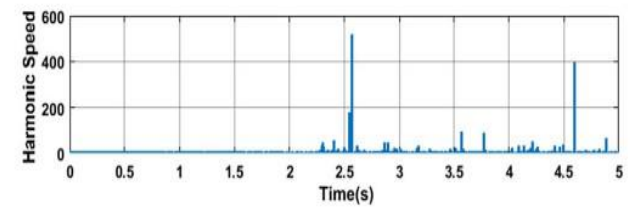


Fig. 12 Harmonic speed waveform of the PID model



DOI: 10.17148/IJIREEICE.2025.131016

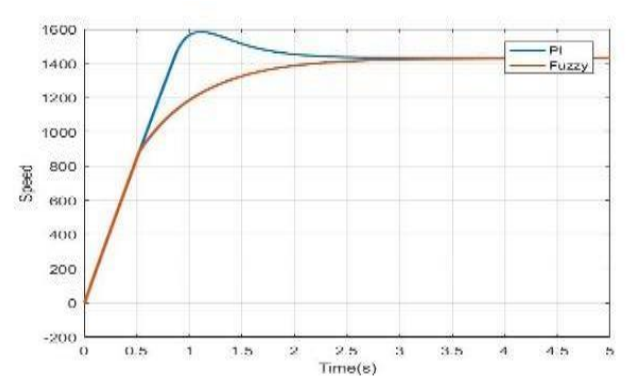


Fig. 14 Speed response comparison for PID and FLC when the reference speed is 1432 rpm

According to the data provided, concerning the magnitude of initial currents, both the temporal response of acceleration and its outputs have shown improvement. The phase current exhibits fewer loss components of the same order when the recommended method is employed. This indicates that the technique reduces speed variation and yields a smoother actual torque [30]. The harmonic speed waveforms for the PID model and the FLC model are illustrated in Figs. 12 and 13, respectively. Both PID and FLC were utilized in various simulation tests to control the IM speed. The speed reference was incrementally adjusted to assess the performance results of the control unit under consistent torque at load, as shown in Figs. 14–16. Table 4 provides a comparison of the performance of FLC and PID in terms of peak overshoot, settling time, and rise time when subjected to multistep speed input. It is clear from Table 4 that FLC offers a quicker response in both settling and rise time compared to PID for multistep speed input, with the exception of the rise time at 1145 (rpm). Consequently, FLC outperformed PID. Additionally, FLC exhibited enhanced control over the speed of the three-phase IM.

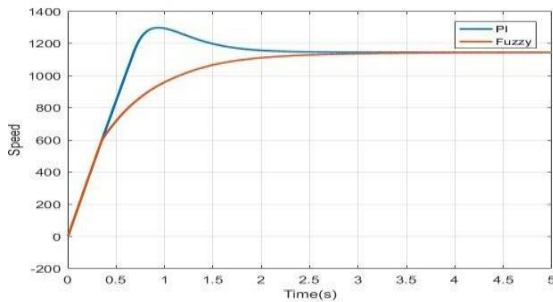


Fig. 15 Speed response comparison for PID and FLC when the reference speed is 1145 rpm

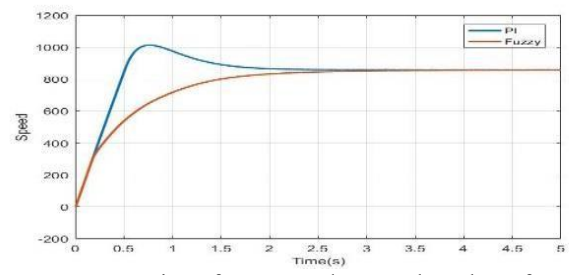


Fig. 16 Speed response comparison for PID and FLC when the reference speed is 859 rpm

PID and FLC were employed in various simulation studies to regulate the IM speed for electric vehicle (EV) applications. The simulations were carried out under a variety of operational parameters, such as applied load and reference speed. The performances of PID and FLC were analyzed and compared. Figures 17a and b depict the speed response of FLC across a spectrum of reference speeds, as well as its performance during a load disturbance. The results of a 20-second simulation are presented in Figure 18. The vehicle comes to a complete halt at time t=0, and the accelerator is suddenly pressed to 70%. The vehicle initiates in electrical mode when the power requirement reaches 10 kW (at t=0.8 s). At t=1.2 s, the brakes are engaged to 70%. This action activates the electric motor to transfer brake energy to the battery and charge it for a duration of four seconds. At time t=1.6 s, the accelerator is abruptly returned to 70% [39].



International Journal of Innovative Research in Electrical, Electronics, Instrumentation and Control Engineering Impact Factor 8.414 

Refereed journal 

Vol. 13, Issue 10, October 2025

#### DOI: 10.17148/IJIREEICE.2025.131016

Table	5	circ	cuit	parameter	S

Item	Parameters	Symbol	Value	Unit
battery	DC input voltage	Vi	780	٧
inverter	snubber resistance	Rs	1000	Ω
	forward voltages	$V_{f}$	0.8	٧
	switching frequency	F <sub>SW</sub>	10	kHz
IM	nominal power	$P_{n}$	37.3	kVA
	voltage (line-line)	$V_{L}$	460	Vrms
	frequency	Fn	60	Hz
	number of poles	P	4	-
	mutual inductance	L <sub>m</sub>	34.7	mH
	stator resistance	Rs	0.087	Ω
	rotor resistance	$R_{\Gamma}$	0.228	Ω
	stator and rotor leakage inductance	$L_{\rm ls} = L_{\rm lr}$	0.8	mH
	moment of inertia	J	1.662	kg m <sup>2</sup>
	rated speed	N	1780	rpm
	friction coefficient	Fc	0.1	Nms
	rated power	Po	50	hp

#### Table 6 Controller parameters

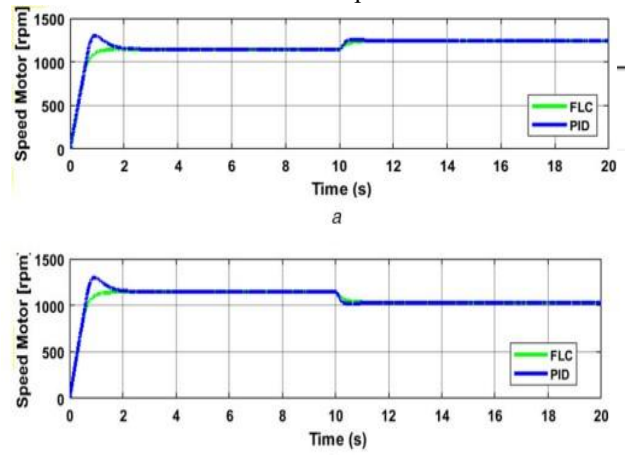


Fig. 17 Speed response comparison for PID and FLC (a), (b) IM response to speed variations ± 100 rpm during 10 s of rated load

b

#### VI. CONCLUSION

Induction motors (IM) may consume more power than necessary when operating below their maximum load capacity. This excess power generates heat. The Fuzzy Logic Controller (FLC) can be employed to manage the amplitude of the initial current, allowing for greater electricity savings during this phase. The fuzzy controller takes as inputs the speed error and the rate of change of the error, which are utilized in the outer loop to formulate an equivalent controller term. This study focused on a simulation of a 50 horsepower IM-driven electric vehicle (EV). Various performance metrics were evaluated, including peak overshoot, steady-state error, rise time, and settling time. The results indicated a reduction in loss components (smaller amplitude) while maintaining the same order components in the phase current of the proposed system. The simulation outcomes of the suggested FLC scheme exhibited remarkable stability and enhanced performance compared to the conventional PID controller, particularly in terms of peak overshoot, rise time, and settling time.

#### REFERENCES

- [1] Sato, E.: 'Permanent magnet synchronous motor drives for hybrid electric vehicles', IEEJ Trans. Electra. Electron. Eng., 2007, 2, (2), pp. 162–168
- [2] Agency, I.E.: 'Global EV outlook 2016: beyond one million electric cars' (OECD Publishing)
- [3] Sayed, K.: 'Zero-voltage soft-switching DC-DC converter-based charger for LV battery in hybrid electric vehicles', IET Power Electron., 2019, 12, (13), pp. 3389–3396
- [4] Gomez, J.C., Morcos, M.M.: 'Impact of EV battery chargers on the power quality of distribution systems',IEEE Power Eng. Rev., 2002, 22, (10), pp. 63–63



## International Journal of Innovative Research in Electrical, Electronics, Instrumentation and Control Engineering Impact Factor 8.414 Refereed journal Vol. 13, Issue 10, October 2025

#### DOI: 10.17148/IJIREEICE.2025.131016

- [5] Stephan, C.H., Sullivan, J.: 'Environmental and energy implications of plug-in hybrid-electric vehicles', Environ. Sci. Technol., 2008, 42, (4), pp. 1185–1190
- [6] Amatani, S., Fukushima, Y., Morita, H.: 'A linear programming based heuristic algorithm for charge and discharge scheduling of electric vehicles in a building energy management system', Omega, 2017, 67, pp. 115–122
- [7] Trove, J.P.F., Roux, M.-A., Menard, E., et al.: 'Energy and power-split management of dual energy storage system for a three-wheel electric vehicle', IEEE Trans. Veh. Technol., 2017, 66, (7), pp. 5540–5550
- [8] Buyukdegirmenci, V.T., Bazzi, A.M., Krein, P.T.: 'Evaluation of induction and permanent-magnet synchronous machines using drive-cycle energy and loss minimization in traction applications', IEEE Trans. Ind. Appl., 2014, 50, (1), pp. 395–403
- [9] Sargonids, A.G., Beni Akar, M.E., Kladis, A.G.: 'Fast adaptive evolutionary PM traction motor optimization based on electric vehicle drive cycle', IEEE Trans. Veh. Technol., 2016, 66, (7), pp. 5762–5774
- [10] Wang, Q., Niu, S., Luo, X.: 'A novel hybrid dual-PM machine excited by AC with DC bias for electric vehicle propulsion', IEEE Trans. Ind. Electron., 2017, 64, (9), pp. 6908–6919
- [11] Bouvardia, S., Daim, S., Matia, A.: 'Sensor fault detection and isolation based on artificial neural networks and fuzzy logic applicated on induction motor for electrical vehicle', Int. J. Power Electron. Drive Syst., 2017, 8, (2), pp. 601–611
- [12] Varghese, S.T., Rajagopal, K.R.: 'Economic and efficient induction motor controller for electric vehicle using improved scalar algorithm'. IEEE 1st Int. Conf. on Power Electronics, Intelligent Control and Energy Systems (ICPEICES), Delhi, 2016, pp. 1–7
- [13] Ulu, C., Korman, O., Komungos, G.: 'Electromagnetic and thermal analysis/ design of an induction motor for electric vehicles. The 8th Int. Conf. on Mechanical and Aerospace Engineering (ICMAE), Prague, 2017, pp. 6–10
- [14] Couchette, A., Abbou, A., Akharas, M., et al.: 'Sensor less direct torque control of induction motor using fuzzy logic controller applied to electric vehicle'. Int. Renewable and Sustainable Energy Conf. (IRSEC), Outrate, 2014, pp. 366–372
- [15] Makrygiorgou, J.J., Alexandridis, A.T.: 'Induction machine driven electric vehicles based on fuzzy logic controllers. The 42nd Annual Conf. of the IEEE Industrial Electronics Society, Florence, 2016, pp. 184–189
- [16] Li, H., Klontz, K.W.: 'Rotor design to reduce secondary winding harmonic loss for induction motor in hybrid electric vehicle application'. IEEE Energy Conversion Congress and Exposition (ECCE), Milwaukee, WI, 2016,pp. 1–6
- [17] Kumar, R., Das, S., Chattopadhyay, A.K.: 'Comparative assessment of two different model reference adaptive system schemes for speed-sensor less control of induction motor drives', IET Electra. Power Appl., 2016, 10, (2),pp. 141–154
- [18] Saleeb, H., Sayed, K., Kassem, A., et al.: 'Power management strategy for battery electric vehicles', IET Electra. Syst. Transp., 2019, 9, (2), pp. 65–74
- [19] Das, S., Pal, A., Manohar, M.: 'Adaptive quadratic interpolation for loss minimization of direct torque- controlled induction motor driven electric vehicle'. IEEE 15th Int. Conf. on Industrial Informatics (INDIN), Emden, 2017, pp. 641–646
- [20] Sayed, K., Abo-Khalil, A.G., Alghamdi, A.S.: 'Optimum resilient operation and control dc microgrid based electric vehicles charging station powered by renewable energy sources', Energies, 2019, 12, (22), p. 4240
- [21] Sayed, K., El-Zohra, E., Naguib, F., et al.: 'Performance evaluations of interleaved ZCS boost DC-DC converters using quasi-resonant switch blocks for PV interface', IOSR J. elector. Electron. Eng., (IOSR-JEEE), 2015, 10, (4), pp. 105–113
- [22] Sayed, K., Gabbar, H.A.: 'Electric vehicle to power grid integration using three-phase three-level AC/DC converter and PI-fuzzy controller', Energies, 2016, 9, p. 532
- [23] Jasim, B.H., Dakhil, A.M.: 'New PI and PID tuning rules using simple analytical procedure'. The Second Scientific Engineering Conf., Mousie, Iraq, 2014
- [24] Lin, W.-S., Huang, C.-L., Chuang, M.-K.: 'Hierarchical fuzzy control for autonomous navigation of wheeled robots', IEE Proc., Control Theory Appl., 2005, 152, (5), pp. 598–606